



Combustion and exergy analysis of multi-component diesel-DME-methanol blends in HCCI engine

Hadi Taghavifar ^{a,*}, Arash Nemati ^{b,**}, Jens Honore Walther ^{b,c}

^a Department of Mechanical Engineering, Faculty of Engineering, Malayer University, Malayer, Iran

^b Department of Mechanical Engineering, Technical University of Denmark, Nils Koppels Allé, 2800 Kgs. Lyngby, Denmark

^c Computational Science and Engineering Laboratory, ETH Zürich, Clausiusstrasse 33, CH-8092 Zürich, Switzerland

ARTICLE INFO

Article history:

Received 9 April 2019

Received in revised form

23 June 2019

Accepted 14 August 2019

Available online 16 August 2019

Keywords:

Exergy estimation

CFD analysis

EGR

HCCI

Multi-component fuel

ABSTRACT

A homogeneous compression ignition (HCCI) engine is taken for numerical investigation on the application of renewable fuels contained blends of methanol and DME with the base diesel fuel, which will be replaced with diesel in different percentages. First, the combustion and engine performance of the engine for two and three-component fuels will be discussed and secondly, the simultaneous effect of EGR in 20% by mass and engine speed in two blends of having maximum and minimum diesel proportion are compared and examined. The results indicate that the replacement of diesel with 20% of DME and 30% by methanol (D50M30DME20) at 1400 rpm generates a greater pressure and accumulated heat (AHR_{peak} = 330.569 J), whereas D80M20/2000 rpm/EGR20 gives a defective combustive performance with poor engine efficiency (IMEP = 7.21 bar). The interesting point is that the proposed optimum blend of D50 can achieve the best performance with 35% mechanical efficiency of 35%. The case of D60M10DME30 though dominates in terms of RPR = 3.177 bar/deg and ignition delay (ID = 4.54 CA) that gives the highest exergy performance coefficient (EPC = 2.063) due to its high work and lowest irreversibility.

© 2019 Elsevier Ltd. All rights reserved.

1. Introduction

It is no more customary to use conventional diesel fuel for CI diesel engines and gasoline for SI engines and engineers through modification and manipulation of fuel composition as emulsions develop new enhanced fuel chemistry, which can be responsible for extra power demand and emission control policies in a global scale. In this framework, adding oxygenated fuels as a substitute with diesel sounds like a pragmatic method to achieve a desirable outcome. Emulsification of different fuels is an idea to balance out the ratio of H–C–O in a blended structure of fuel to give the features of interest. Methanol and Dimethyl ether (DME) are recognized as alcohols in the form of renewable power source in internal combustion engines (ICEs) [1,2] with diverse features that can be replaced by diesel and control the reactivity of air-fuel mixture. Basically, methanol has a very low cetane number and high ignition

delay [3] that can be compensated with the high cetane number of DME. Dimethyl ether has low-ignition temperature [4] and can be easily evaporated with high oxygen content and no C–C bonds [5] contributing to smokeless combustion.

HCCI engines are a new generation of engine systems characterized by low NO_x and high thermal efficiency [6] inheriting the two main capacity of CI and SI engines where there is no direct controlling mechanism over the ignition timing such as injection or spark timing [7]. The use of blended fuels in this kind of engine is more highlighted in HCCI engines since it gives a leverage to determine the ignition timing by modification of alternative fuel fraction with higher/lower flash point thereby tuning the auto-ignition point [8]. The following lists a number of significant studies implemented on the scope of either blended fuels or alternative fuels application in HCCI engines.

Since the operation of HCCI is limited by the ability to control the extreme burning of the homogenous charge and avoiding knock, Li et al. [9] studied the knock phenomenon and cyclic variation within the HCCI engine with a blend prepared by n-butanol and n-heptane. The obtained results indicated that the volume fraction of n-butanol can greatly influence the knock as an increase

* Corresponding author.

** Corresponding author.

E-mail addresses: HadiTaghavifar@yahoo.com (H. Taghavifar), Nemati.arash.mech@gmail.com (A. Nemati).

in butanol lessens the knock probability. Researchers use blending as an outlet to harness the combustion phasing in HCCI ignition mode, for example, Turkcan et al. [10] used a blend of alcohol-gasoline blends in HCCI-DI engine to investigate the impact of second injection timing role on combustion and emission. It was pointed out that increasing methanol fraction would raise the NOx and peak pressure (P_{max}), while an increase of ethanol content works oppositely. Zhang et al. [11] in a study considered exergy losses of the auto-ignition process for DME and alcohol blended fuel. The work indicated that the addition of methanol and DME increases the exergy losses by the H_2O_2 reaction. Wang et al. [12] considered the combustion of polyoxymethylene dimethyl ether (PODE) in an HCCI engine under various EGRs and charge mass equivalence ratios. The detailed data from the study showed that PODE lean HCCI combustion engenders ultra-low NOx and soot content, meanwhile, CO emission decreases with EGR. Yousefzadeh and Jahanian [13] used another alternative fuel in the HCCI engine and proposed compressed natural gas (CNG) to control the combustion phase. Their main findings concluded that hydroxyl radical serves as a robust factor in combustion phasing determination leading to a yet better response time. Nishi et al. [14] were able to set a new HCCI combustion through EGR and engine speed variation. The DME fuel was used in the engine and detailed chemical kinetics was incorporated with a single-zone model. It was shown that higher EGR ratio is required to reach the quasi-steady state. Khandal et al. [15] also tried alternative fuels combustion in HCCI engine. These alternative fuels were Honge biodiesel, cottonseed biodiesel, and hydrogen gas. Their results showed that diesel/biodiesel fuel powered HCCI has 67% lower smoke and 99% lower NOx at 80% load, although 3.4% lower thermal efficiency was reported compared to CI mode. In another recent and relevant study [16], diesel-biodiesel powered HCCI engine was tested that was designed for off-road applications. In brief, the BMEP (brake mean effective pressure) of HCCI without EGR is lower than HCCI with EGR and the BMEP value is the highest for CI engine. Recently, Yao et al. [17] performed a critical review on the diesel-methanol application in CI engines. It was summarized that methanol fumigation can decrease emissions in the diesel engine. The methanol addition to diesel increases the radical pool and the radicals such as H_2O_2 require higher activation energy [18].

Exergy reviews in combustive systems such as engines draw more and more attention due to its potential in identifying the possible agents in reduction of waste energy. In HCCI engines, there are records of exergy study on blended fuels [19–21] where the secondary fuel fraction affects the second law efficiency and heat/work exergy.

From the above review, it can be acknowledged that in HCCI engines it is paramount that the technicians and experts can bring the ignition and combustion phasing under control. So, adopting two alternative fuels with different flammability characteristics, which can substitute diesel by different ratios in a blend seems a logical resolution. Furthermore, EGR introduction in HCCI is practiced to manage the high burning rate of HCCI homogenous charge combustion. Moreover, new exergy terms are used to measure the feasibility of methanol and DME blending in diesel in HCCI mode. The effect of addition of methanol and DME on diesel in HCCI mode combustion is investigated from the second law of thermodynamics view. The numerical work is performed by AVL-FIRE CFD code and then the results of engine modeling are employed for exergy analysis within the framework of in-house developed code. This is a rare work on HCCI engine control by varying DME/methanol on base diesel fuel, which gives flexibility over the ignition and combustion of the engine, meanwhile, a detailed exergetic performance is evaluated with advanced parameters as EGR and secondary fuel fraction changed.

2. Modeling procedure

2.1. Engine modeling with CFD methodology

A TD43 single cylinder, 4-stroke engine operating in lab scale with 600 rpm is selected to simulate an HCCI engine powered by different multi-component renewable fuels (the engine's operational specifications can be found in Table 1). A 1:4 segment of the chamber domain is shown in Fig. 1 with labeled walls in which the flow rme and kinetics of combustion occurs. A meshed view of the chamber at top dead center position consisting of 23K cells is also illustrated in Fig. 1. The boundary conditions of the geometry are the liner wall, moving wall of the piston, head temperatures equal to 475.15, 575.15, 550.15 K.

To implement multi-component fuel combustion, the hydrocarbon fuel is chosen as homogenous multi-component with different percentages from standard species transfer. First, diesel is injected in high ratio and then diesel portion in the blend is reduced and replaced by DME and methanol as alternative fuels.

Diagram flow of different stages of the study from simulation to exergy computations for the case studies is illustrated in Fig. 2.

The model is a closed thermodynamic cycle, therein the IVC is at 120 CA and the EVO at 130 CA. The time step-size is adjusted based on CA- $\Delta\alpha$ division in different stages of engine stroke. The finest step size happens during the combustion period, where detailed chemical and thermodynamic phenomena take place (i.e. $\Delta\alpha = 0.2$). The k-zeta-f [22] is a suitable strategy for modeling the turbulence that can be used in a near-wall area. The three-zone combustion model of ECFM-3Z [23] gives better results especially for multi-component fuels combustion and is applied for this research. For brevity, the adopted sub-models for species transport, combustion, soot, and NOx are listed in Table 2.

The meshing of the computational domain has taken place in ESE diesel platform (AVL-FIRE mesh generation platform), wherein the cells for the spray block are refined to account for two-phase spray combustion. The mean cell size in the meshing is 0.9 mm with a total number of 23900 cells at TDC. In order to examine the predictability of the model and verify the reliability of simulation set-up, the obtained numerical results of the TD43 HCCI engine at 600 rpm for 313 K diesel fuel are contrasted against measured results [24,25]. As Fig. 3 shows, the concordance between numerical and experimental data indicates the acceptable accuracy of the model, hence the veracity of the results generated for multi-component fuels is ensured.

Zang et al. [26] proposed and tested apparent ignition delay correlation that is applicable in the simulation of dual-fuel diesel-methanol powered engines.

$$\tau_{D80M20} = 0.002P^{-2.5}(1 + \phi_{\text{methanol}})^{0.7}\phi_{\text{diesel}}^{-1.04} \exp\left(\frac{4781}{T_b}\right) \quad (1)$$

In addition, Assanis et al. [27] introduced the following equation for diesel fuel:

$$\tau = A\phi^{-0.2}P^{-1.02} \exp\left(\frac{2100}{T}\right) \quad (2)$$

In the above equations, ϕ is the equivalence ratio, T is the initial

Table 1
Engine specification.

| | |
|-----------------------|-------------------------------|
| Bore × stroke | 95 × 82 mm |
| Displacement | 582 cm ³ /cylinder |
| Compression ratio | 18:1 |
| Connecting rod length | 156 mm |

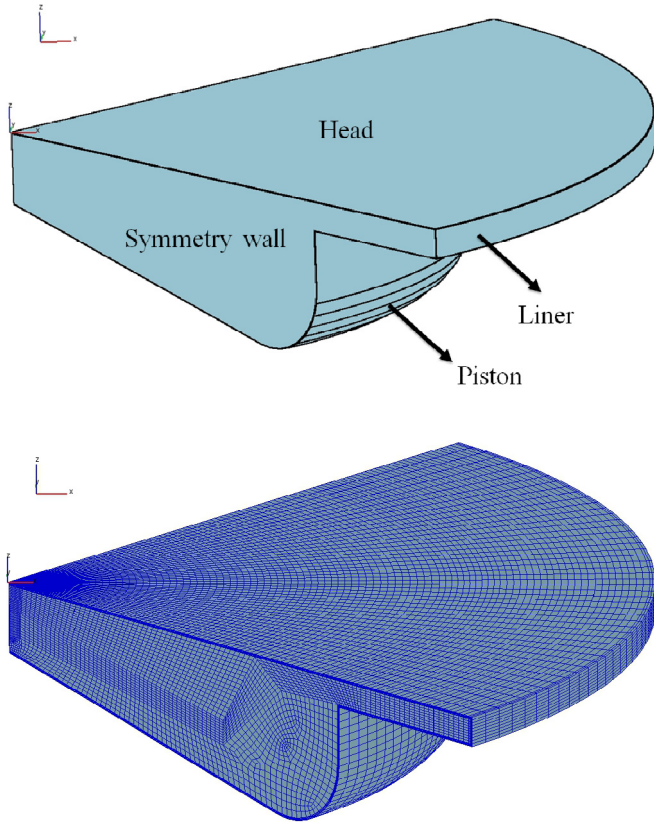
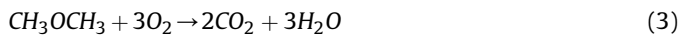


Fig. 1. A quarter domain representation of combustion chamber (labeled and meshed).

temperature, and P represents the in-cylinder pressure. By using the above correlations, and the results of diesel and D80M20, the obtained data are gathered in Table 3 at 600 and 2000 rpm engine speeds.

The final pathway for oxidation of DME is described below (the intermediate detailed reactions are not mentioned) [14]:



and the principal detailed reactions of methanol in the low-

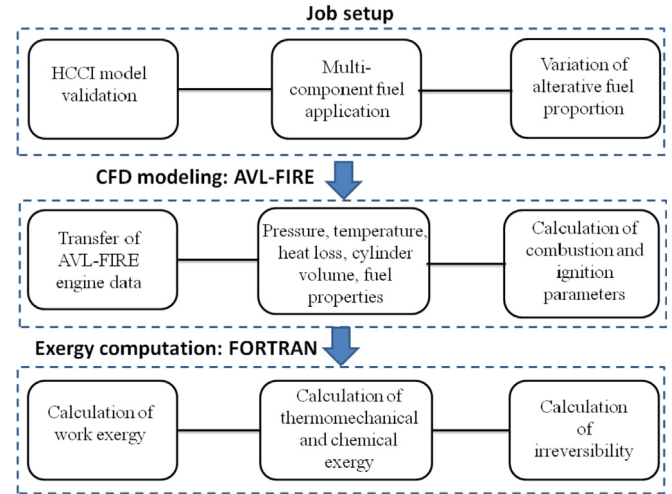


Fig. 2. Flow diagram of interactive simulation-exergy concept in HCCI engine.

Table 2
Applied sub-models in the modeled engine.

| Combustion model | Standard species | NO model | Soot model |
|------------------|------------------|--------------------|---------------|
| ECFM-3Z | Multi-component | Extended Zeldovich | Lund flamelet |



The specification together with physical and chemical characteristics of diesel, DME, and methanol are gathered in Table 4 [4,29,30]. The provided values for different fuels assist towards justification of performance, exergy, and flow behavior of blends.

The fuels in the emulsified state have different combustive, kinetic, and chemical behavior than their pure composition. In the developed code, the calculation of lower heating value (LHV) and the total energy of emulsions are estimated as:

$$\begin{aligned} E_{t, (\text{Diesel-Methanol-DME})} &= \text{LHV}_{\text{Diesel}} \times m_{\text{Diesel}} + \text{LHV}_{\text{Methanol}} \times m_{\text{Methanol}} + \text{LHV}_{\text{DME}} \times m_{\text{DME}} \\ E_{t, (\text{Diesel-Methanol})} &= \text{LHV}_{\text{Diesel}} \times m_{\text{Diesel}} + \text{LHV}_{\text{Methanol}} \times m_{\text{Methanol}} \\ \text{LHV}_{t, (\text{Diesel-Methanol-DME})} &= x_{\text{Diesel}} \times \text{LHV}_{\text{Diesel}} + x_{\text{Methanol}} \times \text{LHV}_{\text{Methanol}} + x_{\text{DME}} \times \text{LHV}_{\text{DME}} \\ \text{LHV}_{t, (\text{Diesel-Methanol})} &= x_{\text{Diesel}} \times \text{LHV}_{\text{Diesel}} + x_{\text{Methanol}} \times \text{LHV}_{\text{Methanol}} \end{aligned} \quad (11)$$

temperature phase (Eqs. (4)–(8)) and high-temperature zone are [28]:

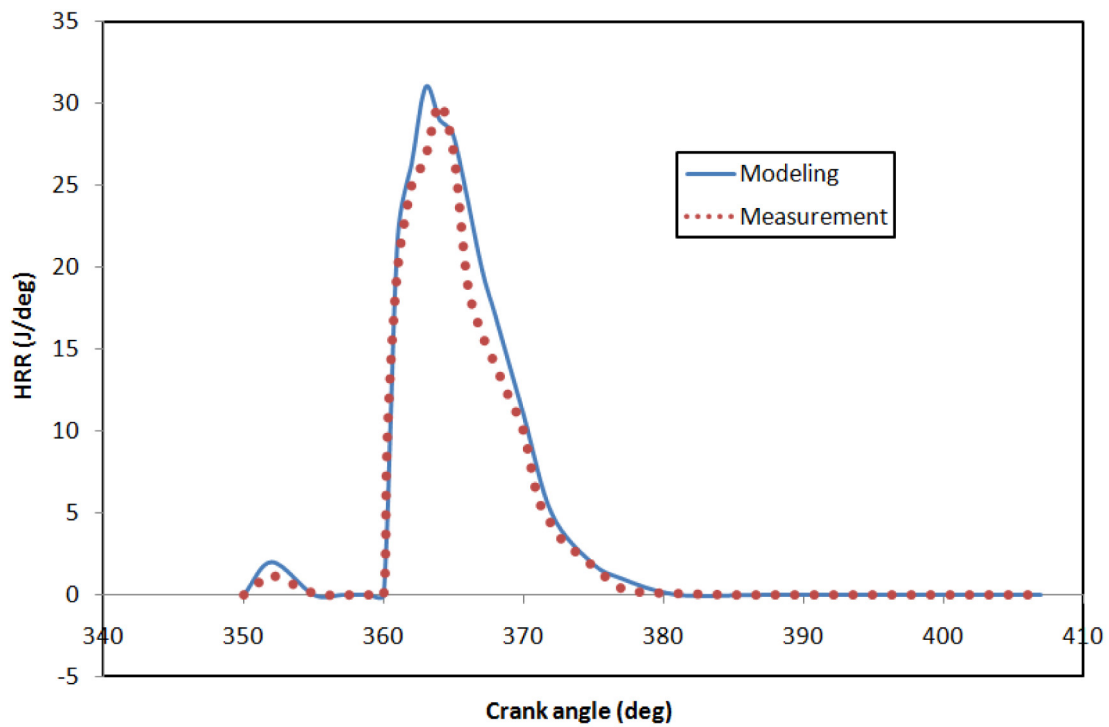


where, E_t represents total energy, LHV is the lower heating value of a specific fuel, m the fuel mass, and x the portion or percentage of fuel in the blend.

2.2. Computation of exergy

The key concept of second-law analysis is 'availability' (or exergy). The availability content of a material represents its potential to do useful work. Unlike energy, exergy can be destroyed which is the result of such phenomena as combustion, friction, mixing, and throttling. The exergy balance in the cylinder can be

(a)



(b)

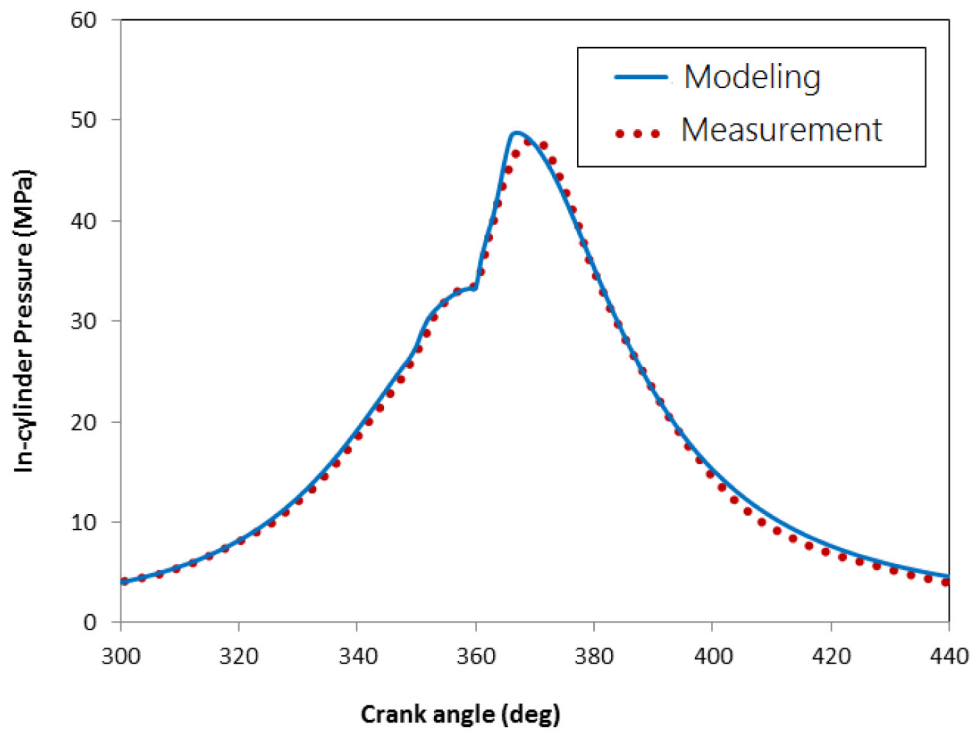


Fig. 3. Validation of the results for TD43 HCCI engine (a) HRR diagram, (b) pressure history at 600 rpm [24,25].

Table 3

Numerical and empirical correlation comparison of ignition delay in CA.

| Engine speed (rpm) | Diesel ID (CA) | | D80M20 ID (CA) | |
|--------------------|----------------|--------------------|----------------|-----------------|
| | Numerical | Assanis Corr. [26] | Numerical | Zang Corr. [27] |
| 600 | 5.1° | 6.0° | 6.3° | 5.8° |
| 2000 | 3.2° | 4.4° | 3.9° | 4.2° |

Table 4

Alternative fuel properties [4,29,30].

| Properties | diesel | methanol | DME |
|----------------------------------|---------------------------------|--------------------|----------------------------------|
| Chemical Formula | C ₁₄ H ₂₅ | CH ₃ OH | CH ₃ OCH ₃ |
| Molecular weight | 179 | 32.04 | 46.07 |
| LHV (MJ/kg) | 42.5 | 20.0 | 28.43 |
| A/F stoichiometric ratio (MJ/kg) | 14.7:1 | 6.43:1 | 9:1 |
| Cetane number | 45.0 | 5.0 | 55–60 |
| Auto-ignition temperature, °C | 210 | 470 | 325 |
| Dynamic viscosity (cSt) | 1–3.97 | 0.543 | 0.185 |
| Oxygen Content, wt% | 0 | 49.93 | 35 |

formulated as follows [31]:

$$\frac{dA_{cyl}}{d\phi} = \frac{\dot{m}_{in}b_{in}^{tm} - \dot{m}_{out}b_{out}^{tm}}{N} - \frac{dA_l}{d\phi} - \frac{dA_w}{d\phi} + \frac{dA_f}{d\phi} - \frac{dI}{d\phi} \quad (12)$$

In the above equation, \dot{m}_{in} and \dot{m}_{out} are the incoming and outgoing flow rates, respectively, b_{in}^{tm} and b_{out}^{tm} refer to their thermo-mechanical exergy which defines as follow [31,32]:

$$b^{tm} = (h - h_0) - T_0(s - s_0) \quad (13)$$

In Equation (12), $\frac{dA_l}{d\phi}$ represents the exergy of heat transfer to the cylinder walls on the basis of crank angle degree. It can be calculated as follow [31,33]:

$$\frac{dA_l}{d\phi} = \frac{dQ_l}{d\phi} \left(1 - \frac{T_0}{T_{cyl}} \right) \quad (14)$$

where, $\frac{dQ_l}{d\phi}$ is the heat transfer rate to the cylinder walls on the basis of crank angle degree and is the instantaneous temperature of the cylinder gasses, which are available from the engine simulation and energy analysis. In the exergy balance equation, the term of $\frac{dA_w}{d\phi}$ represents the indicated work transfer. In fact, it can be defined as the value of output exergy from the cylinder associated with the indicated work [31]:

$$\frac{dA_w}{d\phi} = (P_{cyl} - P_0) \frac{dV}{d\phi} \quad (15)$$

where $\frac{dV}{d\phi}$ states the rate of cylinder volume change based on crank angle degree and P_{cyl} is the instantaneous cylinder pressure which both are calculable by the first law analysis in the engine processes. The burned fuel exergy on the crank angle basis can be calculated as following [31]:

$$\frac{dA_f}{d\phi} = \frac{dm_{fb}}{d\phi} a_{fch} \quad (16)$$

where a_{fch} represents the chemical fuel exergy and for a blend composed of three different fuels this equation can be written as follow:

$$\frac{dA_f}{d\phi} = \frac{dm_{fb1}}{d\phi} a_{fch1} + \frac{dm_{fb2}}{d\phi} a_{fch2} + \frac{dm_{fb3}}{d\phi} a_{fch3} \quad (17)$$

The chemical exergy of substances in the environment (e.g. fuel, sulfur, combustion products such as NO or OH, etc.) can be evaluated by considering an idealized reaction of the substance with others with the known chemical exergies [34]. This chemical exergy of the fuel can be expressed on a molar basis as follow [31,34]:

$$\bar{a}_{fch} = \bar{g}_f(T_0, P_0) - \left(\sum_p x_p \bar{\mu}_p^0 - \sum_r x_r \bar{\mu}_r^0 \right) \quad (18)$$

where index p denotes products (CO₂, H₂O, CO, etc.) and index r is the reactants (fuel and O₂) of the (stoichiometric) combustion process, T_0 and P_0 are the dead state temperature and pressure, and the over bar denotes properties on a mole basis. For liquid fuels of the general type C_zH_yO_pS_q, applicable in internal combustion engines, the chemical exergy of fuel can be expressed as follows (on a kg basis) [35]:

$$a_{fch} = LHV \left(1.0401 + 0.01728 \frac{y}{z} + 0.0432 \frac{p}{z} + 0.2196 \frac{q}{z} \left(1 - 2.0628 \frac{y}{z} \right) \right) \quad (19)$$

The $\frac{dI}{d\phi}$ term in exergy balance equation represents the rate of irreversibility production in the cylinder, which includes combustion, viscous loss, turbulence, mixing, etc.. According to Dunbar and Lior [36], a combustion reaction has four major sources of internal irreversibility. They are:

- A chemical diffusion process in which air and fuel molecules are drawn together.
- Combustion of the fuel-air mixture (thermo-chemical reaction).
- Internal energy exchange through molecular collisions amongst the products and radiation heat transfer amongst product constituents due to unequal heat distribution.
- Mixing process whereby reactants mix before combustion, and products mix with reactants during combustion due to proximity.

Since the contribution of combustion in irreversibility production is more than 90% [37,38], in the present study, only the combustion irreversibility is taken to evaluate the in-cylinder irreversibilities. The combustion irreversibilities on the crank angle basis can be given as [39,40]:

$$\frac{dI}{d\phi} = - \frac{T_0}{T_{cyl}} \sum_j \mu_j \frac{dm_j}{d\phi} \quad (20)$$

where subscript j includes all reactants and products. For ideal gases, $\mu_j = g_j$ and for fuels $\mu_j = a_{fch}$.

Aforementioned equations can be solved by the numerical methods in order to evaluate the second-law terms in an engine cycle.

3. Results and discussion

3.1. Combustion and performance of the engine

Fig. 4 demonstrates the variation trend of turbulent kinetic energy (TKE) for combustion of D50 and D80M20 blends under EGR of 0 and 20%. As shown, the intensity of turbulence for the blend with lower diesel proportion (D50) presents higher TKE amount since an increase of DME and methanol fraction in the blend would increase the flammability of the mixture. The definition of turbulent kinetic energy that is estimated at the initial condition as:

$$TKE = \frac{3}{2} \times U'^2 \left[\frac{m^2}{s^2} \right] \quad (21)$$

$$U' = 0.25 \times (\bar{V}) \left[\frac{m}{s} \right] \quad (22)$$

$$\bar{V} = \frac{2 \times N \times S}{60} \left[\frac{m}{s} \right] \quad (23)$$

where, N denotes the engine speed, V is the mean piston velocity, and S represents the stroke.

Regarding combustion characteristics, the pressure curves of fuel blends are provided in Fig. 5. It is apparent that changing fuel composition has a less significant role than EGR in in-cylinder pressure; in addition, an increase of diesel share in the blend would decrease the pressure at late combustion phase, though the peak pressure is of D60 case. Based on the fuel specifications listed in Table 3, although the heating value of diesel is higher, because the viscosity of DME and methanol are lower, involvement of these alternative fuels would enhance spraying quality. Other reasons for outperformance of blended fuels with decrease of diesel attributes to an addition of oxygen in molecular bond and a balanced ratio of C–O–H in blend composition. The EGR incorporation produces a leaner mixture, which shifts the combustion towards expansion stroke, thus reducing the chamber pressure.

In order to quantify the ignition and combustion quality of the compound fuels, two important parameters are employed as shown in Fig. 5, ignition delay (ID) and rate of pressure rise (RPR) for EGR = 0 and EGR = 20%.

The RPR is calculated in 4 intervals with central differencing derivatives:

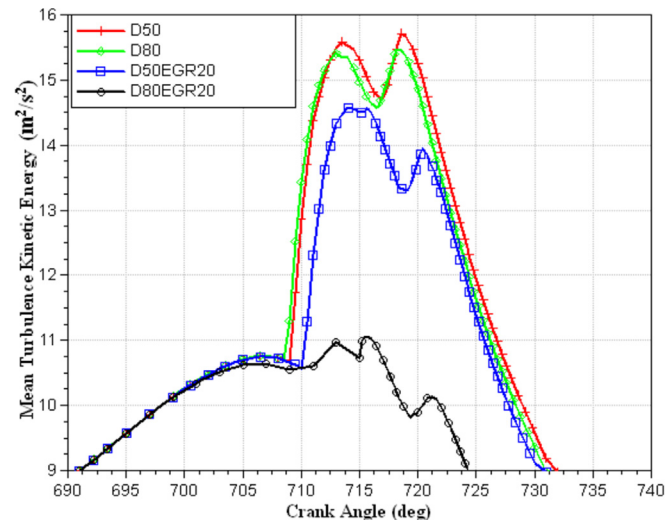


Fig. 4. Variation of TKE vs. CA for high and low diesel fraction with/without EGR.

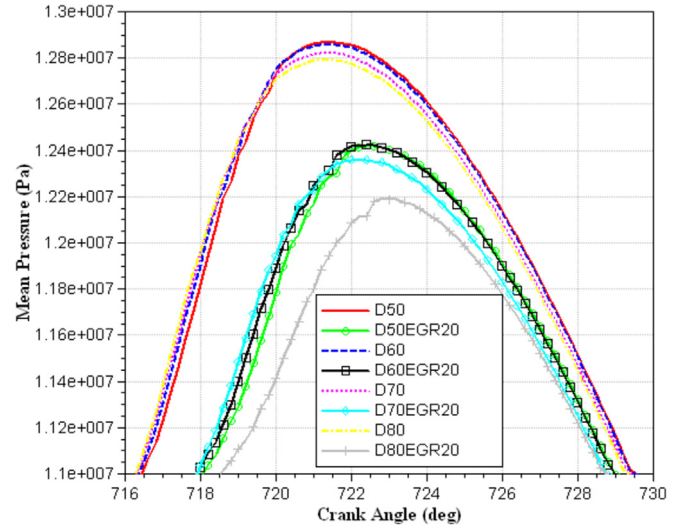


Fig. 5. Pressure history of different blends vs. CA for various fuels with/without EGR.

$$RPR = \frac{dP_i}{d\theta} = \frac{P_{i+2} - P_{i-2}}{4h} \quad (24)$$

P denotes the discrete calculated pressure, h is the change in CA step size between two consecutive runs, so in our case, $h = \Delta\alpha$.

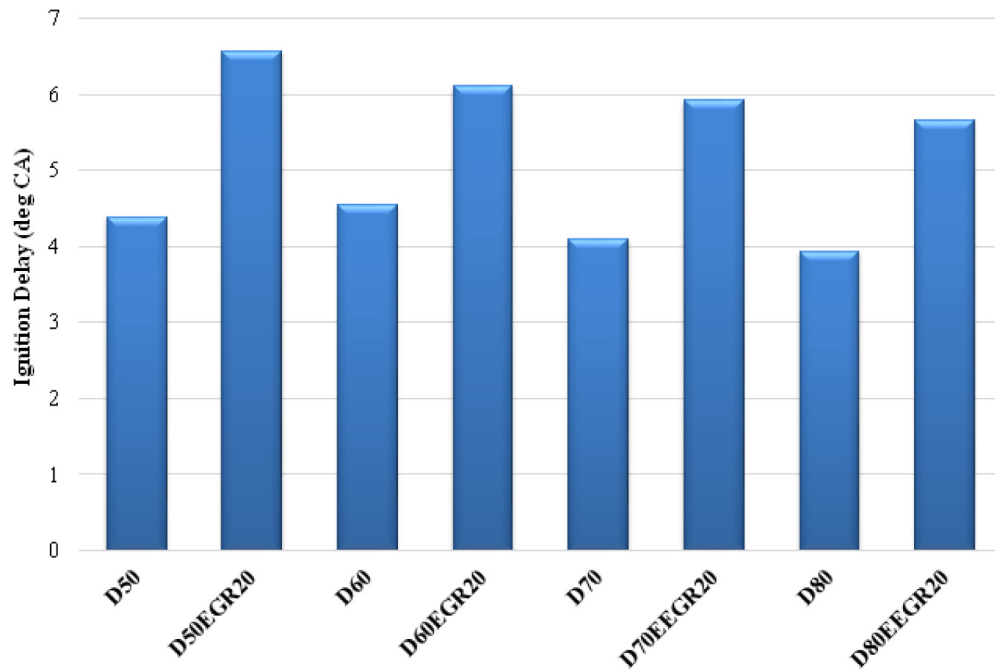
According to Fig. 6a, in total, an increase in diesel share brings about a decreasing trend in ignition delay that can be explained by higher auto-ignition temperatures of replaced fuels i.e., DME and methanol (see Table 4). The max. RPR is plotted in Fig. 6b for different fuel composition and EGR rates. In the presence of EGR addition, increasing diesel share led to higher RPR, while the contrary is happening for the case of no EGR application such that increasing the diesel in the compound fuel composition reduces the RPR. This illustrates that the replacement of diesel with DME and methanol as a three-component blend allows for better reaction with air to boost the pressure in the absence of EGR. The EGR can alleviate sudden pressure rise and knock probability of blends containing methanol and DME.

Fig. 7 shows the heat release rate (HRR) curves of different blended fuels for different operational modes. The peak HRR as seen belongs to D50 that as expected is in concordance with RPR results since this composition generated the highest-pressure jump and instantaneous heat generation due to oxygen involvement in the molecular structure of DME and methanol. The key point is that when EGR is included, the HRR of different blends shows different behavior, and D80M20 is dominant, while in the absence of EGR, the peak HRR reaches 59.49 J/deg for D50.

For further illustration of heat generation of different multi-component fuels, Fig. 8 is presented. Again as shown in Fig. 8, the EGR = 20% application led to a significant decrease of accumulated heat release (AHR) for all blended fuels and as diesel share decreases in the blend, the AHR increases as well. This is primarily because the methanol and DME are low-viscous liquids, which can be disintegrated easily and ameliorate the spray and mixing process. The secondary reason goes to high cetane number of DME (55–60), which improves the flammability and ignition index of the blend.

Another important combustion parameter is the in-cylinder temperature that is plotted with and without EGR consideration in Fig. 9. Due to the dilution effect of EGR, the temperature is dropped for all the fuels and increasing the diesel proportion (from D50 to D80M20) in the blend caused a slight decrease in the

(a)



(b)

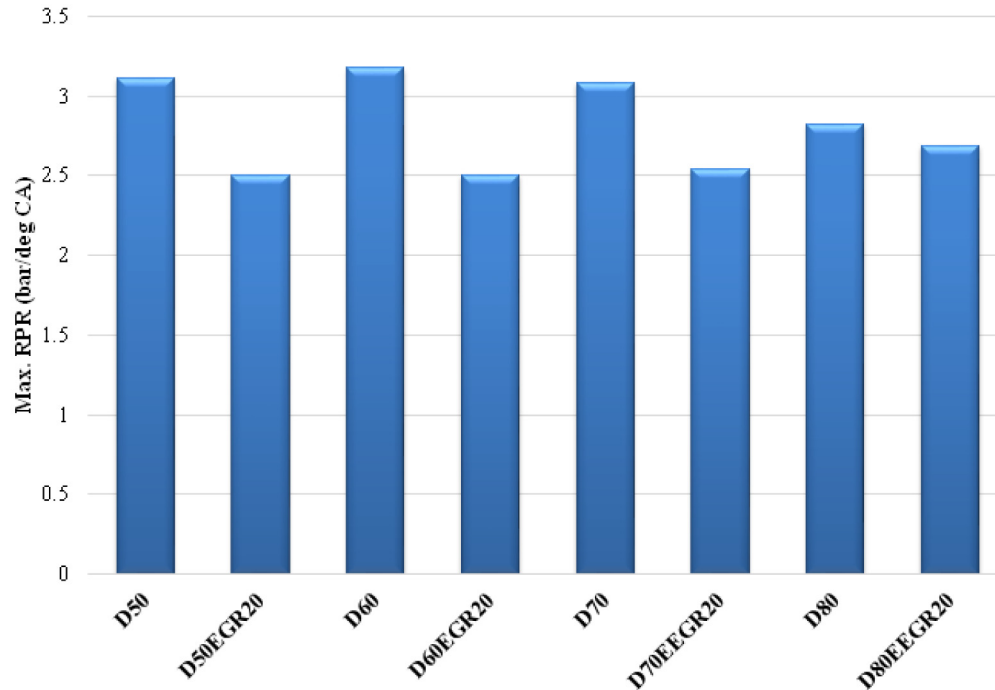


Fig. 6. (a) Ignition delay for different blended fuel composition for EGR = 0 and EGR = 20%, (b) Max. RPR for different blended fuel composition for EGR = 0 and EGR = 20%.

temperature. Moreover, adding methanol and DME increase the oxygen content, which will improve the oxidation of hydrocarbons and would definitely increase the chamber temperature.

The wall heat-flux diagram for different fuels and EGR effects is

shown in Fig. 10. The minimum and maximum heat flux of the wall pertains to D80M20/EGR20 and D50 with -10855 W and -13420 W , respectively. The more heat-flux of D50 is associated with better spraying characteristics and inherent combustion

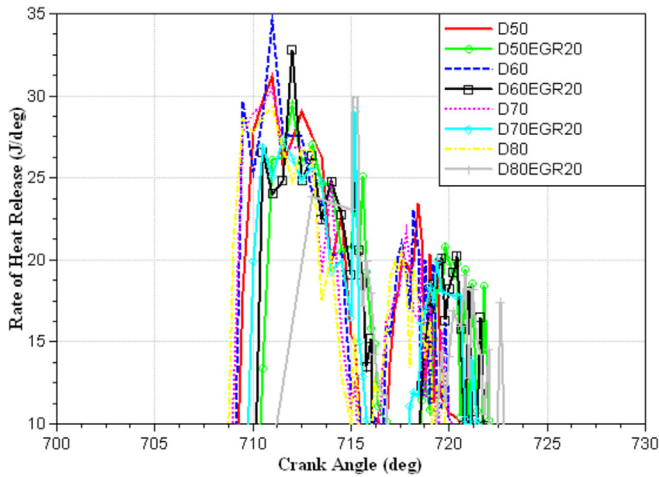


Fig. 7. HRR curves vs. CA for different fuel blends with/without EGR.

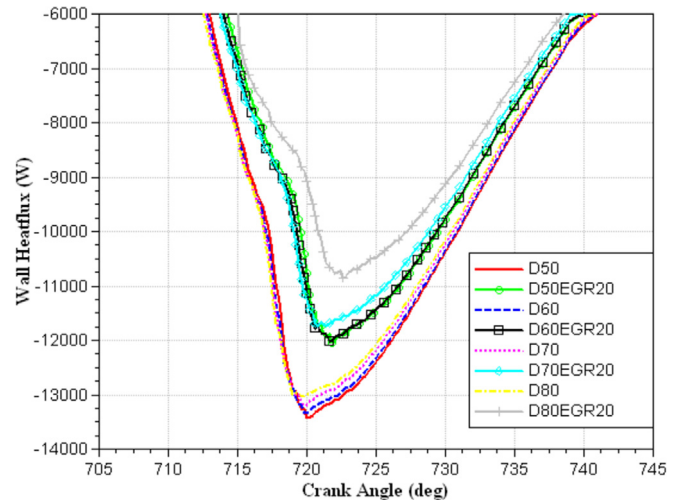


Fig. 10. Wall heat flux vs. CA for different blends with/without EGR.

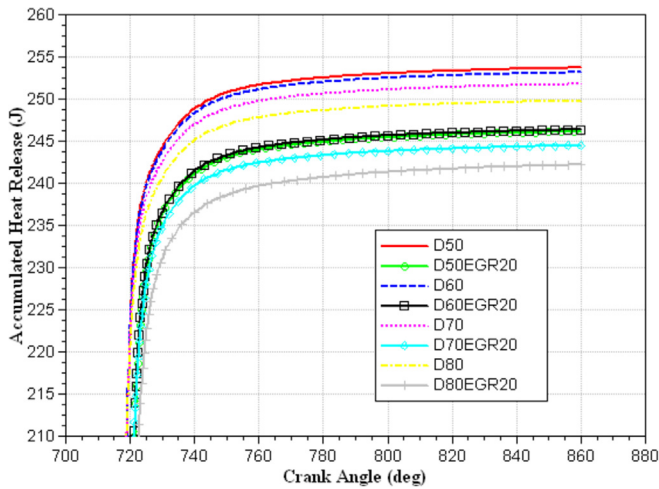


Fig. 8. AHR of different blends vs. CA, various fuels with/without EGR.

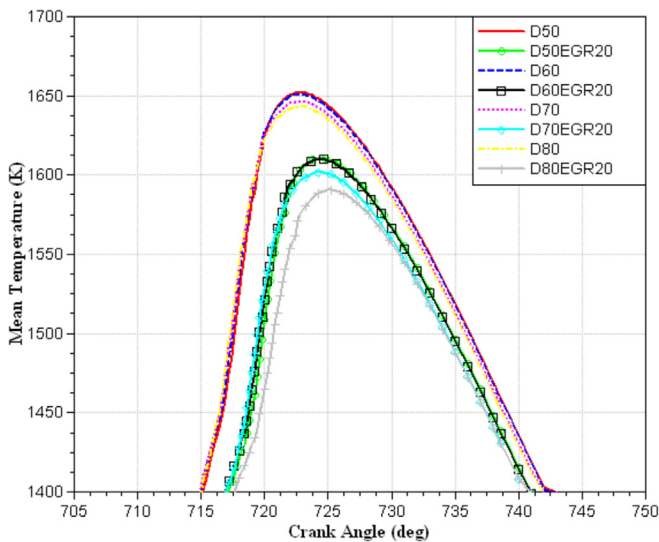


Fig. 9. In-cylinder temperature vs. CA for different blends with/without EGR.

qualities of blended fuel with more percentage of methanol and DME.

Table 5 is provided to present the performance and efficiency of the HCCI engine for different fuel compositions under different engine speeds and EGR levels. First of all, it can be observed that D50 with 35% efficiency is the most efficient blend as other performance metrics such as indicated power and indicated torque are also greater, since in-cylinder pressure and heat generation for it is sensibly superior than other blends. Second, for a given blend EGR as predicted would reduce the performance adversely and lead to a debilitated engine functionality as for D70, EGR = 20% has reduced indicated torque (IT) from 18.41 N m to 17.08 N m. As the results indicate, the engine operation at low speed of 1400 rpm would decrease the engine efficiency, although IT and IMEP increased for any of the blends.

The CO emission results are depicted in Fig. 11 with variable fuel composition versus CA. It is evident that the low-concentration of NO_x specie occurs with D50 and the spatial distribution of CO along the wall edge is decreased in this case. The rich CO content along the wall boundary layer is due to incomplete combustion. Besides, It is obvious that the D50 composition is ideal for CO reduction due to rich oxygen content of the blend found in DME and methanol. This oxygen presence accelerate the CO oxidation to CO₂ and the more DME and methanol replacement with diesel in the blend, the more oxidation and more CO reduction takes place. The increase of DME and ethanol share adds a more balanced C–H bond i.e. lower carbon in the blend, thus the CO formation can be decreased due to chemical reaction during the post-combustion period.

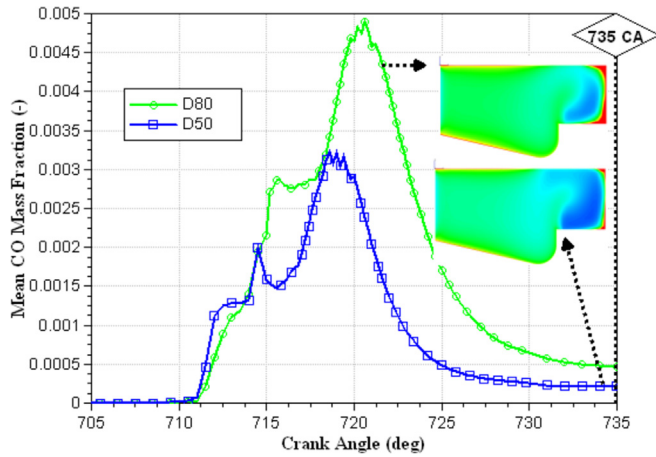
3.2. Exergy and irreversibility evaluation

Availability of blended fuel energy in HCCI mode is a critical topic that has close ties with chemistry and combustion kinetics. The sources of irreversibilities when various fractions of burnt fuel can give an insight on exergy destruction factors. Fig. 12 exhibits the thermo-mechanical and accumulative irreversibility graphs with CA for different blends composition. On account of higher pressure and temperature curves for D50, higher thermo-mechanical exergy is seen for this case and EGR acts as a factor to reduce the power density. The increment of oxygenated methanol and DME fuels leads to complete oxidation and release of more chemical energy. This leads to combustion prolonging and the exhaust gases' thermo-mechanical exergy increment as can be seen in Fig. 12 a.

Table 5

Performance of HCCI for blended multi-component fuels at rated engine speeds.

| | N = 2000 rpm | | | | | | | | N = 1400 rpm | | | |
|------------|--------------|--------|-------|--------|----------|----------|----------|----------|--------------|--------|----------|----------|
| | D50 | D60 | D70 | D80 | D50EGR20 | D60EGR20 | D70EGR20 | D80EGR20 | D50 | D80 | D50EGR20 | D80EGR20 |
| IMEP (bar) | 7.6 | 7.57 | 7.52 | 7.48 | 7.36 | 7.32 | 7.26 | 7.21 | 7.87 | 7.77 | 7.75 | 7.64 |
| IP (kW) | 3.95 | 3.92 | 3.85 | 3.81 | 3.68 | 3.65 | 3.58 | 3.52 | 2.97 | 2.89 | 2.88 | 2.79 |
| IT (N.m) | 18.87 | 18.69 | 18.41 | 18.2 | 17.59 | 17.39 | 17.08 | 16.83 | 20.23 | 19.71 | 19.65 | 19.06 |
| η (%) | 35% | 34.40% | 34% | 33.60% | 32.87% | 32.55% | 32% | 31.70% | 26.30% | 25.60% | 25.40% | 24.30% |

**Fig. 11.** CO variation vs. CA for different blends.

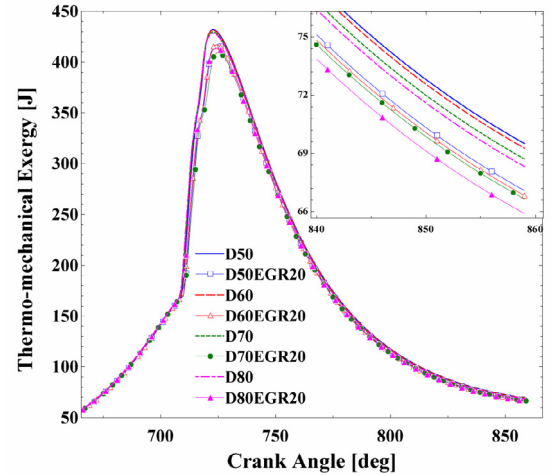
For irreversibility, the highest and lowest amounts belong to D80 and D60, respectively. According to Eq. (20), there are three significant parameters, which have a dominant influence on the combustion irreversibility including in-cylinder gases temperature, chemical exergy, and the combustion rate. One of the key parameters, which affect irreversibility, is the chemical exergy of fuels. The chemical exergy of fuel is directly related to its LHV and according to Table 4, diesel fuel has the highest LHV and chemical exergy, followed by DME and methanol. Therefore, D80 with the highest amount of diesel in its composition and the lowest in-cylinder temperature has the highest amount of irreversibility.

Two main exergy parameters including heat loss exergy and indicated work exergy reduced to burned fuel exergy (as a percentage of burned fuel exergy) are represented in Fig. 13. Based on Fig. 13 a., the heat loss exergy for the cases with 0% EGR is higher than that of cases with 20% EGR. The lowest heat loss exergy reduced to fuel exergy belongs to D80EGR20 with 10.68%. As seen in this figure, the percentage of heat loss exergy for D50 is lower than those of D60, D70, and D80. This is because, despite the wall heat flux for D50 is higher than others (according to Fig. 10), but the burned fuel exergy for this blend is higher which leads to this trend. As seen in Fig. 13 b, the cases with 20% EGR have higher indicated work exergy reduced to burned fuel exergy than the cases without EGR. The main reason for this trend is lower burned fuel exergy due to incomplete combustion in the presence of EGR despite the higher indicated work exergy in the cases without EGR. This means the cases with EGR transfer higher portion of burned fuel exergy as indicated work.

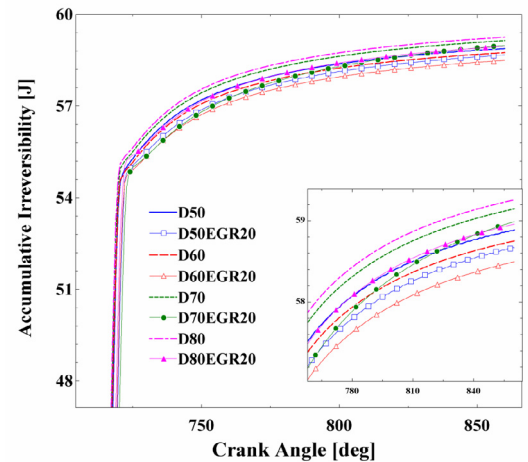
A key parameter, known as exergetic performance coefficient (EPC), is taken into account recently to evaluate the energy performance and exergy output simultaneously. Calculation of this index is given as:

$$EPC = \frac{\text{Indicated Work}}{\text{Irreversibility}} \quad (25)$$

(a)



(b)



1

Fig. 12. (a) Thermo-mechanical exergy and (b) accumulative exergy for different blends and exergy.

In the above relation, there is a competition between output indicated work (determined by heating value and mean effective pressure) with irreversibility (determined by the degree of combustion). The best compromise can be reached for D60 as plotted in Fig. 14. In other words, D60 has more total exergy and exhibits the lowest irreversibility, as a result, the EPC fraction is the highest for D60 case.

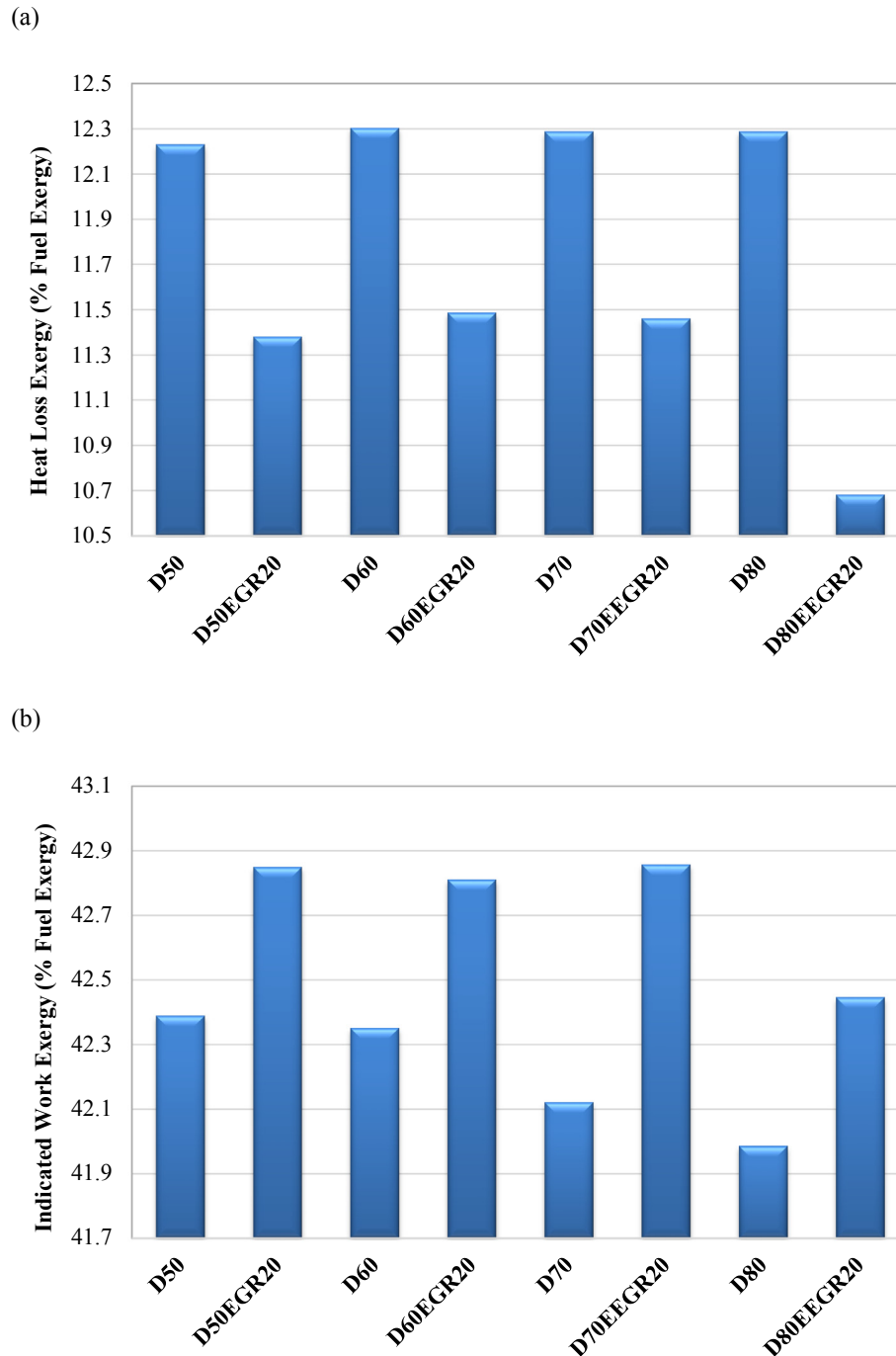


Fig. 13. Variation of (a) heat loss exergy and (b) indicated work exergy reduced to burned fuel exergy for different blend composition and EGR rates.

4. Conclusion

It is of great interest to concoct and synthesize fuel blends that can cope with the demand to both increase the engine power and reduce the emission at the same time. This study investigated four fuel blends of D50M30DME20, D60M10DME30, D70M20DME10, and D80M20 in an HCCI engine for with/without EGR application. As the following remarks would confirm, D50M30DME20 is an ideal solution to boost the energetic performance, while D60M10DME30 dominates in terms of exergy performance and lower irreversibility:

- i. The D50 powered HCCI engine with EGR = 20% has the maximum ID and minimum RPR, while increasing diesel fraction in blend decreases ID monotonically and increases RPR. When no EGR is used, D60 (representative of highest DME fraction in the blend) has both maximum ID and RPR. It shows that EGR alters the pattern of ID and RPR trends for proposed multi-component fuels.
- ii. Due to higher cetane number of DME (~60), the blend with the highest ratio percentage of DME (D60) represents the highest ID (4.546 CA) and RPR (3.177 bar/deg CA), which results in high HRR. These are owing to the low viscosity of DME and longer ID, which remarkably improves the mixture

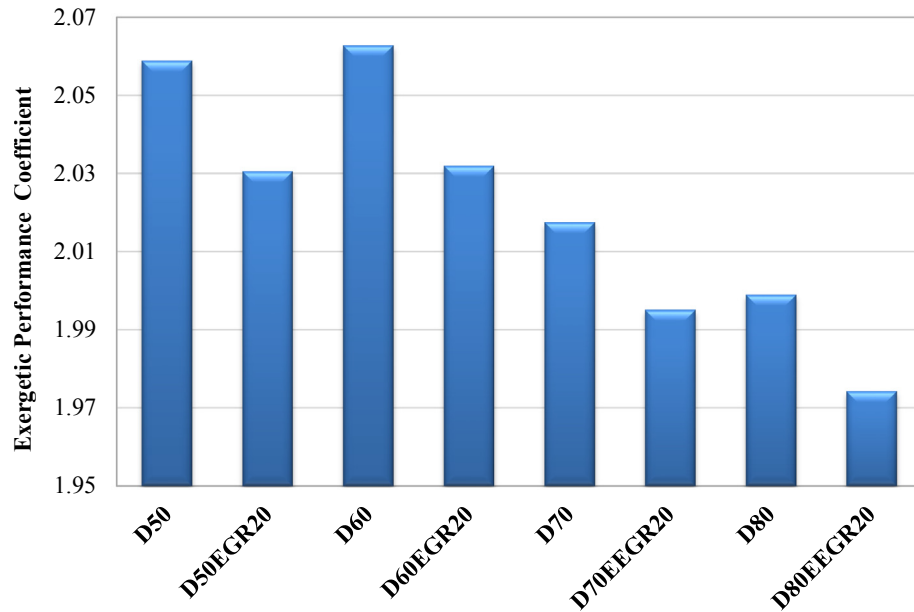


Fig. 14. Variation of EPC for different blend composition and EGR rates.

uniformity. When EGR is involved, the scale of intense burning rate for this blend is suppressed.

- iii. The case of D60 has the lowest irreversibility rate and ranks second in exergy terms that leads to identifying it with the highest EPC. On the other hand, D80 with the highest portion of diesel fuel in its composition (80%), shows the worst energetic and exergetic performance among the blends.
- iv. It was revealed that in engine performance terms (IMEP, IP, IT, efficiency), D50 among other blends is dominant in both 1400 rpm and 2000 rpm speeds. As known EGR would decrease the engine's performance and efficiency and higher engine speed definitely increases the engine output power. The closure statement is that there found a potential candidate solution (i.e. D50 powered HCCI engine) that can simultaneously increase the engine efficiency and decrease the irreversibility.

References

- [1] Sorenson SC, Glensvig M, Abata DL. Dimethyl ether in diesel fuel injection systems (No. 981159. SAE Technical Paper; 1998.
- [2] Soni DK, Gupta R. Application of nano emulsion method in a methanol powered diesel engine. *Energy* 2017;126:638–48.
- [3] De Caro PS, Mouloungui Z, Vaitilingom G, Berge JC. Interest of combining an additive with diesel–ethanol blends for use in diesel engines. *Fuel* 2001;80(4):565–74.
- [4] Park SH, Lee CS. Applicability of dimethyl ether (DME) in a compression ignition engine as an alternative fuel. *Energy Convers Manag* 2014;86: 848–63.
- [5] Arcoumanis C, Bae C, Crookes R, Kinoshita E. The potential of di-methyl ether (DME) as an alternative fuel for compression-ignition engines: a review. *Fuel* 2008;87(7):1014–30.
- [6] Liu MB, He BQ, Zhao H. Effect of air dilution and effective compression ratio on the combustion characteristics of a HCCI (homogeneous charge compression ignition) engine fuelled with n-butanol. *Energy* 2015;85:296–303.
- [7] Chen Y, Wolk B, Mehl M, Cheng WK, Chen JY, Dibble RW. Development of a reduced chemical mechanism targeted for a 5-component gasoline surrogate: a case study on the heat release nature in a GCI engine. *Combust Flame* 2017;178:268–76.
- [8] Maurya RK, Akhil N. Numerical investigation of ethanol fuelled HCCI engine using stochastic reactor model. Part 2: parametric study of performance and emissions characteristics using new reduced ethanol oxidation mechanism. *Energy Convers Manag* 2016;121:55–70.
- [9] Li G, Zhang C, Zhou J. Study on the knock tendency and cyclical variations of a HCCI engine fuelled with n-butanol/n-heptane blends. *Energy Convers Manag* 2017;133:548–57.
- [10] Turkcan A, Altinkurt MD, Coskun G, Canakci M. Numerical and experimental investigations of the effects of the second injection timing and alcohol-gasoline fuel blends on combustion and emissions of an HCCI-DI engine. *Fuel-Guildford* 2018;219(1):50–61.
- [11] Zhang J, Huang Z, Han D. Exergy losses in auto-ignition processes of DME and alcohol blends. *Fuel* 2018;229:116–25.
- [12] Wang Z, Liu H, Ma X, Wang J, Shuai S, Reitz RD. Homogeneous charge compression ignition (HCCI) combustion of polyoxymethylene dimethyl ethers (PODE). *Fuel* 2016;183:206–13.
- [13] Yousefzadeh A, Jahanian O. Using detailed chemical kinetics 3D-CFD model to investigate combustion phase of a CNG-HCCI engine according to control strategy requirements. *Energy Convers Manag* 2017;133:524–34.
- [14] Nishi M, Kanehara M, Iida N. Assessment for innovative combustion on HCCI engine by controlling EGR ratio and engine speed. *Appl Therm Eng* 2016;99: 42–60.
- [15] Khandal SV, Banapurmath NR, Gaitonde VN. Performance studies on homogeneous charge compression ignition (HCCI) engine powered with alternative fuels. *Renew Energy* 2019;132:683–93.
- [16] Godiño JAV, Aguilar FJJE, García MT. Simulation of HCCI combustion in air-cooled off-road engines fuelled with diesel and biodiesel. *J Energy Inst* 2018;91(4):549–62.
- [17] Yao C, Pan W, Yao A. Methanol fumigation in compression-ignition engines: a critical review of recent academic and technological developments. *Fuel* 2017;209:713–32.
- [18] Xu GL, Yao CD, Rutland CJ. Simulations of diesel–methanol dual-fuel engine combustion with large eddy simulation and Reynolds-averaged Navier–Stokes model. *Int J Engine Res* 2014;15(6):751–69.
- [19] Neshat E, Saray RK, Hosseini V. Investigation of the effect of reformer gas on PRFs HCCI combustion based on exergy analysis. *Int J Hydrogen Energy* 2016;41(7):4278–95.
- [20] Nemati P, Jafarmadar S, Taghavifar H. Exergy analysis of biodiesel combustion in a direct injection compression ignition (CI) engine using quasi-dimensional multi-zone model. *Energy* 2016;115:528–38.
- [21] Amjad AK, Saray RK, Mahmoudi SMS, Rahimi A. Availability analysis of n-heptane and natural gas blends combustion in HCCI engines. *Energy* 2011;36(12):6900–9.
- [22] Hanjalic K, Popovac M, Hadziabdic M. A robust near-wall elliptic-relaxation eddy-viscosity turbulence model for CFD. *Int J Heat Fluid Flow* 2004;25: 1047–51.
- [23] Colin O, Benkenida A. The 3-zones extended coherent flame model (ECFM3Z) for computing premixed/diffusion combustion. *Oil Gas Sci Technol* 2004;59(6):593–609.
- [24] Ebrahimi R, Desmet B. An experimental investigation on engine speed and cyclic dispersion in an HCCI engine. *Fuel* 2010;89(8):2149–56.
- [25] Mansoury M, Jafarmadar S, Talei M, Lashkarpour SM. Optimization of HCCI (Homogeneous Charge Compression Ignition) engine combustion chamber walls temperature to achieve optimum IMEP using LHS and Nelder Mead algorithm. *Energy* 2017;119:938–49.
- [26] Zang R, Yao C, Yin Z, Geng P, Hu J, Wu T. Mechanistic study of ignition characteristics of diesel/methanol and diesel/methane dual fuel engine. *Energy Fuels* 2016;30(10):8630–7.
- [27] Assanis DN, Filipi ZS, Fiveland SB, Syrimis M. A predictive ignition delay

- correlation under steady-state and transient operation of a direct injection diesel engine. *J Eng Gas Turbines Power* 2003;125(2):450–7.
- [28] Westbrook CK, Dryer FL. Comprehensive mechanism for methanol oxidation. *Combust Sci Technol* 1979;20(3–4):125–40.
- [22] Varol Y, Öner C, Öztöpe HF, Altun Ş. Comparison of methanol, ethanol, or n-butanol blending with unleaded gasoline on exhaust emissions of an SI engine. *Energy Sources, Part A Recovery, Util Environ Eff* 2014;36(9):938–48.
- [29] Park SH, Lee CS. Combustion performance and emission reduction characteristics of automotive DME engine system. *Prog Energy Combust Sci* 2013;39(1):147–68.
- [30] Soni DK, Gupta R. Optimization of methanol powered diesel engine: a CFD approach. *Appl Therm Eng* 2016;106:390–8.
- [31] Haywood RW. Equilibrium thermodynamics for engineers and scientists. 1980.
- [32] Taghavifar H, Nemati A, Salvador FJ, De la Morena J. Improved mixture quality by advanced dual-nozzle, included-angle split injection in HSDI engine: exergetic exploration. *Energy* 2019;167:211–23.
- [33] Nemati A, Barzegar R, Khalilarya S. The effects of injected fuel temperature on exergy balance under the various operating loads in a DI diesel engine. *Int J Exergy* 2015;17(1):35–53.
- [34] Bejan A. Advanced engineering thermodynamics. John Wiley & Sons; 2016.
- [35] Stepanov VS. Chemical energies and exergies of fuels. *Energy* 1995;20(3):235–42.
- [36] Dunbar WR, Lior N. Sources of combustion irreversibility. *Combust Sci Technol* 1994;103(1–6):41–61.
- [37] Rakopoulos CD, Giakoumis EG. Second-law analyses applied to internal combustion engines operation. *Prog Energy Combust Sci* 2006;32(1):2–47.
- [38] Alkidas AC. The application of availability and energy balances to a diesel engine. *J Eng Gas Turbines Power* 1988;110(3):462–9.
- [39] Nemati A, Fathi V, Barzegar R, Khalilarya S. Numerical investigation of the effect of injection timing under various equivalence ratios on energy and exergy terms in a direct injection SI hydrogen fueled engine. *Int J Hydrogen Energy* 2013;38(2):1189–99.
- [40] Rakopoulos CD, Andritsakis EC. DI and IDI diesel engines combustion irreversibility analysis. In: American society of mechanical engineers-winter

annual meeting; 1993. p. 17–32. New Orleans, Louisiana, U.S.A., 1993.

Abbreviation

AHR: accumulated heat release (J)
 ATDC: after top dead center
 BD: biodiesel-diesel
 B50D50: 50% biodiesel, 50% diesel shares by volume
 CA: crank-angle
 D100: pure diesel
 D50: Diesel(50%)Methanol(30%)DME(20%)
 D60: Diesel(60%)Methanol(10%)DME(30%)
 D70: Diesel(70%)Methanol(20%)DME(10%)
 D80: Diesel(80%)Methanol(20%)
 DME: Dimethyl ether
 E_t: total energy
 ECFM-3Z: extended coherent flame method-3 zone
 ED: ethanol-diesel
 EGR: exhaust gas recirculation
 EPC: exergetic performance coefficient
 EVO: exhaust valve opening
 HRR: heat release rate (J/deg)
 HCCI: homogenous charge compression ignition
 ID: ignition delay (deg CA)
 IMEP: indicated mean effective pressure (bar)
 IP: indicated power (kW)
 IT: indicated torque (N.m)
 IVC: intake valve closing
 LHV: lower heating value (MJ/kg)
 RPR: rate of pressure rise (bar/deg)
 TKE: turbulent kinetic energy (m²/s²)
 V: mean piston velocity (m/s)
 η: efficiency